International Journal of Mechanical, Industrial and Aerospace Sciences
ISSN: 2517-9950
Vol:14, No:2, 2020

Kinetic Parameter Estimation from Thermogravimetry and Microscale Combustion Calorimetry

Rhoda Afriyie Mensah, Lin Jiang, Solomon Asante-Okyere, Xu Qiang, Cong Jin

***Abstract*—**Flammability analysis of extruded polystyrene (XPS) has become crucial due to its utilization as insulation material for energy efficient buildings. Using the Kissinger-Akahira-Sunose and Flynn-Wall-Ozawa methods, the degradation kinetics of two pure XPS from the local market, red and grey ones, were obtained from the results of thermogravity analysis (TG) and microscale combustion calorimetry (MCC) experiments performed under the same heating rates. From the experiments, it was discovered that red XPS released more heat than grey XPS and both materials showed two mass loss stages. Consequently, the kinetic parameters for red XPS were higher than grey XPS. A comparative evaluation of activation energies from MCC and TG showed an insignificant degree of deviation signifying an equivalent apparent activation energy from both methods. However, different activation energy profiles as a result of the different chemical pathways were presented when the dependencies of the activation energies on extent of conversion for TG and MCC were compared.

***Keywords*—**Flammability, microscale combustion calorimetry, thermogravity analysis, thermal degradation, kinetic analysis.

I. Introduction

TG analysis measures the mass loss of pyrolyzing materials as a function of time and temperature under controlled heating rates lower than 60 ^{o}C/min. During the experiment, the sample mass is kept smaller and the heating rates, lower to ensure a uniform temperature gradient [1], [2]. It is noteworthy that increasing the heating rate of the TG experiment tends to move the mass loss to higher temperatures. The TG analysis coupled with differential thermogravimetry (DTG) results is typically applied to mathematically define the thermal decomposition kinetics of the pyrolysis of the solid-phase material [3], [4]. Kinetic parameter estimation could be performed based on a single or multiple heating rate results. Multiple heating rate method with a minimum of four iso-heating rate mass loss curves is preferred since it establishes the dependence of chemical reactions on heating rate and produces model-specific reaction parameters that are significant at all heating rates [5].

Using the afore-mentioned approach, Jiang et al. [6] analyzed the pyrolysis behavior of waste XPS from TG experiments performed at 5 ^{o}C/min, 10 ^{o}C/min, 15 ^{o}C/min and 20 ^{o}C/min heating rates.

The authors calculated the activation energy required for pyrolysis using several iso-conversional methods. From their research, the dependence of activation energy on the extent of conversion (α) was found to be in three regions. Thus, an increase in E_a from 140 – 170 kJ/mol at $\alpha < 0.2$, E_a stabilizes at 180 kJ/mol from $0.2 < \alpha \leq 0.8$ and increases rapidly with an increase in α. Similarly, Jiao et al. [7] conducted a thermal degradation study on pure XPS samples at 5 ^{o}C/min, 10 ^{o}C/min, 20 ^{o}C/min and 30^{o}C/min heating rates. In their work, the Kissinger-Akahira-Sunose (KAS) method was applied in estimating the activation energy of XPS sample in inert and oxidizing atmosphere. Under nitrogen atmosphere, it was observed from their study that E_a increased rapidly at lower conversions, maintained an approximate constant of 165 kJ/mol between the conversion range $\alpha = 0.15$ - 0.9 and at ($\alpha >$ 0.9), the value decreased to 149.24 kJ/mol.

The activation energy describes the minimum number of elementary reactions that define the decomposition process [4], [8]. Due to the complexity of the thermal degradation of XPS, it is quite clearly seen that different activation energy profiles have been presented in literature. In spite of the usefulness of TG technique in pyrolysis studies, the heating rate applied is usually lower than the estimated heating rate for polymer pyrolysis [9]. Increasing the heating rate of the TG experiment beyond the stipulated limits of the apparatus whiles keeping a uniform temperature gradient within the sample has been explored in this study. The effects of elevated heating rates on the activation energy for the pyrolysis of XPS samples have also been analyzed.

It is worth noting that, MCC can also be applied to study the thermal degradation kinetics of polymers. Unlike TG, MCC combines pyrolysis, combustion and char production mechanism which is a very important flammability reduction method. Therefore, to describe the kinetics of the thermal degradation of char forming polymers it is necessary to adopt the MCC. MCC provides information on the heat release rate as a function of temperature or time as well as the heat of combustion [9]-[14].

Snegirev et al. [15], [16] conducted kinetic analysis on the pyrolysis of polystyrene in non-oxidizing atmosphere with zero char yield. The kinetic parameters obtained were similar to the TG results in literature. They also sought to identify the most appropriate kinetic model to derive the kinetic

R. A. Mensah is with the School of Mechanical Engineering, Nanjing University of Science and Technology, 210094 Nanjing, China (phone: +8613151566950; e-mail: ramensah@ymail.com).
L. Jiang, the School of Mechanical Engineering, Nanjing University of Science and Technology, 210094 Nanjing, China (phone: +86 25 84317023; e-mail: jianglin@ustc.edu.cn).
X. Qiang is with the School of Mechanical Engineering, Nanjing University of Science and Technology, 210094 Nanjing, China (phone: +8613404160644; e-mail: xuqiang@njust.edu.cn).
S. Asante-Okyere is with the School of Mechanical Engineering, Nanjing University of Science and Technology, 210094 Nanjing, China (phone: +8618801590962; e-mail: solomon@njust.edu.cn).
C. Jin is with the School of computer Engineering, Nanjing University of Science and Technology, 210094 Nanjing, China.

parameters of polystyrene degradation using data from MCC. Results from their work proved that all the adopted models produced similar results.

A comparative study was conducted on the thermal degradation of XPS samples using TG and MCC experiments in this study. This was done by estimating kinetic parameters of XPS pyrolysis through MCC and comparing the estimated activation energy with that of thermogravimetric analysis at the same heating rates. To ensure consistency and accuracy of the activation energy, two iso-conversional methods, KAS and Flynn-Wall-Ozawa methods, were compared. The significance of the finding is in the degree of deviation between the activation energy obtained from MCC and TG techniques.

II. Experimental Kinetic Methods

A. Materials

The flammability of pure red and grey XPS obtained from Zheng bang Newly Building Material Co. Ltd. in China was studied. The samples were cut from large boards of XPS into milligram sizes for the experiments. The Mettler AX-205 Analytical Semi Micro Balance Delta Range with a readability of 0.01 mg and a weighing range of 81 g was used to weigh the samples. The material properties are shown in Table I.

TABLE I
PROPERTIES OF XPS

Property	Red	Grey
Thermal conductivity /$Wm^{-1}K^{-1}$	0.1316	0.1357
Thermal diffusivity /$m^2\ s^{-1}$	0.4201	0.4401
Specific heat capacity /kJ $g^{-1}\ K^{-1}$	1.34	1.39
LOI %	19.3	20.5
Density, $\boldsymbol{\rho}$/ kg m^{-3}	52.6	37.8
Density of molten material, $\boldsymbol{\rho}$/ kg m^{-3}	828	806

B. TG Analysis

The thermal degradation of red and grey XPS was studied by simultaneous thermal analysis using Netzsch STA 449C TG experiment. The TG experiment was performed in accordance with the standard procedures in ASTM 1641-16 [2], [3]. Samples of 5 mg were placed in a crucible and heated in a furnace at constant heating rates. The heating rates selected were 0.1 K s^{-1}, 0.2 K s^{-1}, 0.5 K s^{-1}, 1.0 K s^{-1}, 1.5 K s^{-1}, 2.0 K s^{-1}, 2.5 K s^{-1}, 3.0 K s^{-1}, and 3.5 K s^{-1} in nitrogen atmosphere with a flow rate of 60 mL min^{-1}. The nitrogen gas was Instrument Nitrogen 5.0 purchased from AGA industrial gases. The rate of mass loss as a function of time and temperature was measured and recorded.

C. MCC

The MCC experiment took place at the VTT Technical research center of Finland in an MCC-2 equipment from Govmark Limited. According to standards in ASTM D7309-13 [17], the experimental procedure applied was in line with Method A. Milligram samples taken from XPS boards were weighed and prepared for the MCC experiment. Samples of mass ranging from 1 mg to 4 mg were heated at a temperature of 75°C to 600°C in a pyrolyzer under a heating rates ranging from 0.1 K $s^{-1}$to 3.5 K s^{-1}. The volatile pyrolysis products were removed from the pyrolyzer by nitrogen gas and oxidized with excess oxygen at 900°C in a tubular combustion furnace. Oxygen consumption calorimetry was applied in calculating the heat release rate from the volumetric flow rate and oxygen concentration of the gases that flowed out of the combustor [14], [18]. Three replicate prepared samples were tested and an average of the measured results was recorded. The samples were labelled as xps_1_0.1 representing the first sample tested under 0.1 K s^{-1} and so on. The heat release temperature, time to heat release and heat release rate were measured and recorded.

D. Kinetic Theory

The chemical reaction equilibrium states that, the rate of reaction of a chemical process is proportional to the concentration of reactants used per unit time. This is written as (1) [19]:

$$\frac{d\alpha}{dt} = k(T)f(\alpha) \tag{1}$$

where $\frac{d\alpha}{dt}$ is the reaction rate, $f(\alpha)$ is the concentration of reactants and $k(T)$, the rate constant at absolute temperature. The rate of reaction of the pyrolysis of a material is dependent on temperature. The temperature dependence is defined by the Arrhenius equation developed by Svante Arrhenius in 1884 [20]:

$$k(T)=A\exp\left[-\frac{E_a}{RT}\right] \tag{2}$$

where, R is the universal gas constant and T represents the absolute temperature. Equation (3) establishes a relationship between the Arrhenius equation and rate of reaction.

$$\frac{d\alpha}{dt}=Af(\alpha)e^{-\frac{E_a}{RT}} \tag{3}$$

where, α is the conversion rate which ranges from 0 to 1. It is estimated by using (4) where m_o, m, and m_f are the initial, current and final mass of the sample [6].

$$\alpha=\frac{(m_O-m)}{(m_O-m_f)} \tag{4}$$

Writing (3) in terms of heating rate gives (5):

$$\frac{d\alpha}{dt}=\frac{A}{\beta}f(\alpha)e^{-\frac{E_a}{RT}} \tag{5}$$

Equation (5) can also be written as:

$$\frac{d\alpha}{f(\alpha)}=\frac{A}{\beta}e^{-\frac{E_a}{RT}dT} \tag{6}$$

Integrating and rearranging (6) result in:

$$g(\alpha)=\int_0^{\alpha}\frac{d\alpha}{f(\alpha)}=\frac{A}{\beta}\int_{T_0}^{T}e^{\frac{-E_a}{RT}}dT \tag{7}$$

Substituting $x=\left[\frac{E_a}{RT}\right]$ in (7) gives:

$$p(x)=\int_x^{\infty}\frac{e^{-x}}{x^2}dx \tag{8}$$

The integrated form of the conversion function, $g(\alpha)$ can thus, be solved as follows [21]:

$$g(\alpha)=\frac{AE_a}{\beta R}\int_x^{\infty}\frac{e^{-x}}{x^2}dx \Rightarrow g(\alpha)=\frac{AE_a}{\beta R}p(x) \tag{9}$$

Taking the natural logarithm of (9) results in:

$$\ln(g(\alpha))=\ln\left(\frac{AR}{E_a}\right)+\ln\left(\frac{1}{\beta}\right)+\ln(p(x)) \tag{10}$$

With Doyle's approximation, $\ln(p(x))=-2.315-0.4567x$ and for all $\frac{E_a}{RT}>20$, the integral can be approximated to obtain (11).

$$\ln(\beta)=\ln\left(\frac{AE_a}{Rg(\alpha)}\right)-2.135-0.4567\frac{E_a}{RT} \tag{11}$$

where g(α) is the integral form of kinetic model (i.e., $g(\alpha)=kt$). Hence, by plotting $\ln(\beta)$ against $\left(\frac{1}{T}\right)$, E_a and A can be calculated from the slope and intercept, respectively. Thus,

$$E_a\approx-\frac{R}{0.4567}\cdot\frac{\Delta\ln(\beta)}{\Delta T^{-1}} \tag{12}$$

Equation (11) represents the Flynn-Wall-Ozawa (FWO) method. With the FWO method, the activation energy values are a function of only heating rate [22]. Similarly, from (9), the variables A and E_a are independent of T whereas A and E_a are independent of α. Further integration of (9) gives:

$$\ln g(\alpha)=\ln\left(\frac{AE_a}{R}\right)-\ln\beta+\ln p(x) \tag{13}$$

The KAS can hence be defined as:

$$\ln\left(\frac{\beta}{T^2}\right)=\ln\left(\frac{AR}{E_a g(\alpha)}\right)-\frac{E_a}{RT} \tag{14}$$

Therefore, plotting $\ln\left[\frac{\beta}{T^2}\right]$ against $\left[\frac{1}{T}\right]$ for a constant value of α yields a straight line with the slope and y-intercept being $\left[\frac{-E_a}{R}\right]$ and $\ln\left[\frac{AR}{g(\alpha)E_a}\right]$, respectively. E_a and A can be thus, calculated from the results [19], [20].

E. Derivation of Peak Reaction Rate [r_p] from MCC Data

The end products pyrolysis process of XPS is solid residue and volatile gases. This can be written as (15) [15], [16]:

$$m_o=v_r m_o+(1-v_r)m_o \tag{15}$$

The mass of solid residue m_f of the sample is expressed in terms of char yield (v_r) as:

$$m_f=v_r m_o \tag{16}$$

The rate of gasification is equivalent to the rate of mass loss $-\frac{dm}{dt}$, with m being the current mass of the sample. Heat release rate ($\dot{q}$) equals heat of combustion (Δq) multiplied by the mass loss rate. Therefore, the heat release rate per unit mass can be written as:

$$\dot{q}=\Delta q\left(-\frac{1}{m_o}\frac{dm}{dt}\right) \tag{17}$$

Substituting the first derivative of (16) and (17) simplifies (18).

$$\dot{q}=\Delta q(1-v_r)\frac{d\alpha}{dt} \tag{18}$$

Let $\frac{d\alpha}{dt}=r$. r can be expressed in terms of heat release rate as: $r=\frac{\dot{q}}{\Delta q''}$ with the heat of combustion per unit mass of the sample ($\Delta q''$) written as:

$$\Delta q''=\Delta q(1-v_r) \tag{19}$$

r_p represents the peak reaction rate $\left(\frac{d\alpha}{dt}\right)_{\max}$ for the experiment and it is identical in TG and MCC if the heat of combustion per unit mass of the original sample is equal to the integral heat of combustion per unit mass of the original sample and it is constant throughout the process [15], [16]. Conversion is obtained by integrating the reaction rate at constant heating rates as shown in (20).

$$\alpha=\frac{1}{\beta\Delta q''}\int_{T_0}^{T}\dot{q}(T)dT \tag{20}$$

Alternatively, the mass loss rate $-\frac{dm}{dt}$ in (17) can be expressed in terms of rate constant as:

$$-\frac{dm}{dt}=k(T)(m-v_r m_o) \tag{21}$$

where k(T) represents the pyrolysis reaction rate constant defined in (2). Using a constant heating rate and integrating the mass loss rate at to attain the current mass of sample at a specific temperature T results in (22).

$$\frac{m(T)}{m_o}=v_r+(1-v_r)e^{-y} \tag{22}$$

$$y=\frac{ART^2\exp\left[-\frac{E_a}{RT}\right]}{\beta(E_a+2RT)} \tag{23}$$

A combination of (21) and (22) gives the specific mass loss rate at a constant heating rate, β.

$$-\frac{1}{m_0}\frac{dm}{dt}=(1-v_r)k(T)e^{-y} \tag{24}$$

By equating the second derivative of (22) to zero with an initial condition of $(v_r\neq 1)$, the reaction rate constant at the peak mass loss rate temperature, T_p can be written as:

$$k(T)_{\max}=\frac{\beta E_a}{RT_p^2} \tag{25}$$

Substituting (25) into (24) produces the peak reaction rate which is also equivalent to the maximum specific mass loss rate of the sample [23].

$$r_p=\left(-\frac{1}{m_o}\frac{dm}{dt}\right)_{\max}=\frac{\beta(1-v_r)E_a}{e^y RT_p^2}\approx\frac{\beta(1-v_r)E_a}{eRT_p^2} \tag{26}$$

III. Results and Discussion

A. TG Analysis

The TG and DTG curves for red and grey XPS conducted under nitrogen are shown in Figs. 1 and 2. The plots show a total of nine curves corresponding to the nine heating rates selected for the experiment. The mass loss of the XPS samples began at 200 °C and increased gradually to the peak. It can be observed from the curves that both red and grey XPS showed two peaks signifying two weight loss stages. It should be noted that the first peak is more defined in red XPS than grey XPS. In the degradation of red XPS, the first stage of weight loss occurred between the temperatures of 260 °C to 315 °C whiles the second stage happened between 415 °C and 460 °C. Similarly, with grey XPS the first and second stages of weight loss occurred at 342 °C to 375 °C and 419 °C to 483 °C, respectively for nine heating rates. The general trend observed as seen in the degradation process of most polymeric materials was that the peak temperature increased with increasing heating rate.

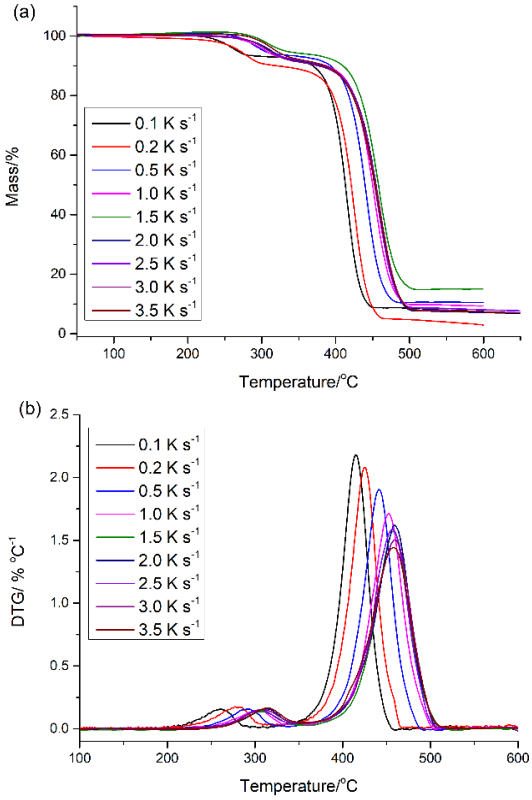

Fig. 1 TG (a) and DTG (b) results for red XPS

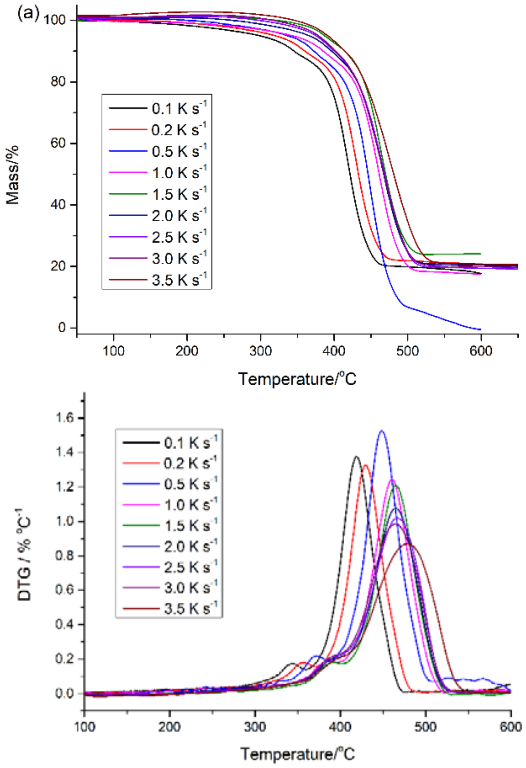

Fig. 2 TG (a) and DTG (b) results for grey XPS

The highest mass loss rate was recorded at a heating rate of 0.2 K s^{-1} for red and 0.5 K s^{-1} for grey XPS. Also, the residual mass obtained for red XPS was smaller as compared to grey XPS.

B. MCC Analysis

The specific heat release rate of red and grey XPS measured during the MCC experiment was plotted against temperature in Figs. 3 and 4. Like the TG results, the peak temperature increases with increasing heating rate. Similar peak temperatures were observed at the same heating rate for both materials. The heat release rate of red XPS was almost twice that of grey XPS [14].

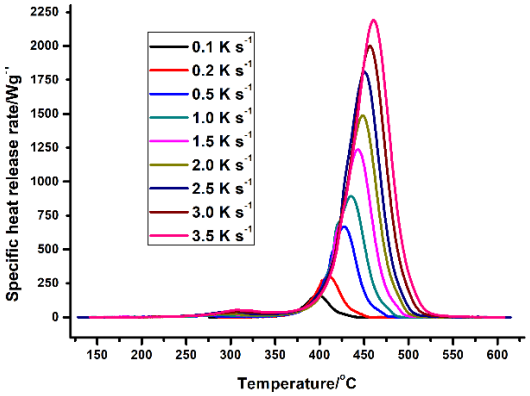

Fig. 3 Specific heat release rate versus temperature for red XPS

C. Kinetic Analysis

The experimental results from TG and MCC showing the temperatures at initial (T_o), peak (T_p), and final (T_f) reactions were recorded for red and grey XPS. The heat release rate, heat of combustion, char yield, and the calculated peaak reaction rate from the MCC experiments are listed in Tables II and III. Both experiments were performed under the same heating rates. An illustration of the means of locating T_o, T_p and T_f is shown in Fig. 5. The initial temperature was obtained by extrapolating the onset of the shift in the mass loss curve which corresponds to the beginning of the first peak on the DTG curve to the temperature axis. The peak temperature was determined by the temperature corresponding to the highest peak on the DTG curve.

Averagely, T_p for grey XPS was higher than red XPS. An observation was also made that T_p was higher in TG than MCC. Materials that display a single step decomposition reaction such as polystyrene produce similar TG and MCC results [24]. Hence, the peak reaction rate for the samples can be determined from any of the experiments.

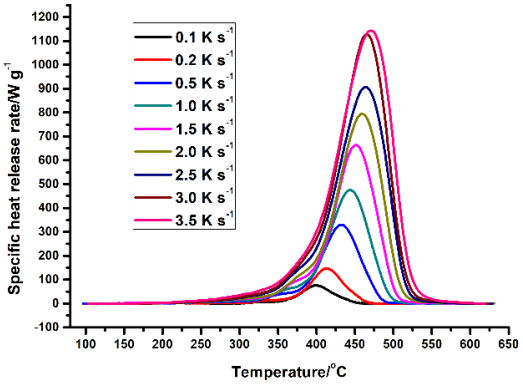

Fig. 4 Specific heat release rate versus temperature for grey XPS

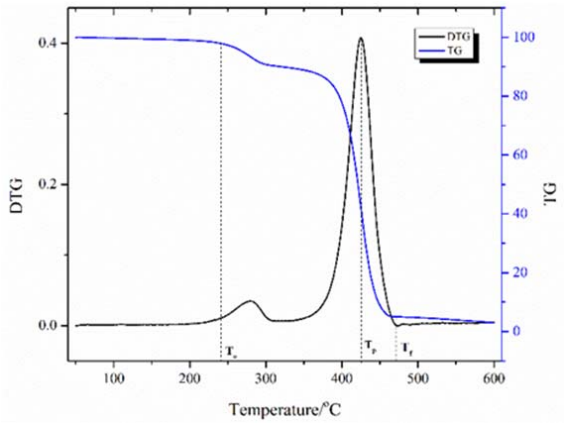

Fig. 5 Determination of decomposition characteristic temperatures T_o, T_p and T_f

TABLE II
RED XPS RESULTS FROM MCC AND TG EXPERIMENTS

β/ K s^{-1}	T_p/°C		T_o/°C		T_f/°C		$\dot{q}$ W g^{-1}	Δq kJ g^{-1}	v_r	r_p /s^{-1}
	TG	MCC	TG	MCC	TG	MCC				
0.1	415.57±6.5	397.9±9.9	264±5.3	373±8.4	450±9.5	415±2.4	163±9	32.4±0.07	0.006849	0.00507
0.2	425.39±0.2	410.4±1.3	270±8.4	384±8.9	463±6	432±2.2	300.6±15.58	31±1.5	0.059211	0.01031
0.5	441.48±6.3	428.2±6.3	297±6.3	388±6.1	478±4.5	446±9.5	668±31.56	34.5±1.8	0.014493	0.01965
1.0	452.25±4.1	435.8±6.1	306±8	403±8.8	483±2.2	458±7.7	948.8±25.4	33.2±0.5	0.02	0.02916
1.5	458.52±1.3	442.9±5.2	333±6.4	405±6.8	505±9.2	466±2.6	1236.5±54.1	33.3±0.5	0.034483	0.03846
2.0	461.23±1.4	447.8±3.1	317±4.6	407±4.3	500±2.2	471±1.5	1488.4±63.2	32.1±0.7	0.101351	0.0516
2.5	457.58±6.5	451±2.6	312±9.0	411±5.6	498±6.6	476±2.8	1809±64.8	33±0.08	0.058824	0.05824
3.0	461.32±0.6	455.7±3.2	310±8.5	420±4.5	493±5.3	482±3.9	1999.8±93	32.8±0.2	0.080537	0.06631
3.5	459.35±3.5	460.5±3.7	320±7.7	418±8.9	504±4.8	483±7.7	2192±85	32.5±0.5	0.078014	0.07315

TABLE III
GREY XPS RESULTS FROM MCC AND TG EXPERIMENTS

β K s^{-1}	T_p/°C		T_o/°C		T_f/°C		$\dot{q}$ W g^{-1}	Δq kJ g^{-1}	v_r	r_p /s^{-1}
	TG	MCC	TG	MCC	TG	MCC				
0.1	419.12±8.7	402±7	340±5.3	363±3.1	460±7.8	429±8.4	79.2±5.8	25.5±0.02	0.115646	0.00292
0.2	429.89±1.2	412.4±0.5	358±8	366±3	480±9	441±5.9	149.5±9.2	24.1±1.5	0.170732	0.00748
0.5	447.75±7.5	432.1±8.3	370±6.3	364±6.9	500±5.3	461±2.9	339±11.8	25.3±0.6	0.098361	0.01486
1.0	461.23±8.2	443.2±3.9	386±8.4	375±8.4	498±5.3	472±4.4	533±23.3	26.7±0.3	0.136986	0.02313
1.5	465.62±2.8	451±0.4	413±6.4	384±5.9	513±4.5	481±9.8	728.7±22.1	30.1±3.3	0.019868	0.02832
2.0	464.79±4.8	456.3±3.7	396±4.9	391±7.6	516±7.1	487±3.6	806.4±26.3	27.4±0.09	0.131387	0.03525
2.5	468.34±4.9	462.1±3.1	399±9	385±7.9	520±8.2	493±5.4	977.5±31.7	27.4±0.4	0.182353	0.04174
3.0	467.5±6.5	467.6±0.6	402±5.1	393±5.8	525±8.4	495±7.5	1062.3±28.9	27.8±0.4	0.162921	0.04565
3.5	479.1±7.5	473.4±2	417±6.2	392±9.7	530±6.2	499±5.1	1206.6±36.8	28±0.7	0.136364	0.0499

TABLE IV
THE DEPENDENCE OF E_a ON A FROM TG ANALYSIS

Conversion	Red XPS			Grey XPS		
	E_a/kJ mol^{-1}	Standard error	R^2	E_a/kJ mol^{-1}	Standard error	R^2
0.1	95.348	2.09	0.995	157.264	1.5	0.996
0.15	128.766	4.48	0.990	219.614	2.2	0.995
0.2	212.271	3.2	0.994	252.852	2.7	0.994
0.25	251.814	3.7	0.993	279.090	2.3	0,996
0.3	278.391	2.7	0.994	271.086	1.9	0.997
0.35	313.322	3.2	0.995	270.983	1.8	0.997
0.4	317.265	2.5	0.996	269.110	1.8	0.998
0.45	313.322	2.4	0.996	260.960	1.7	0.997
0.5	305.978	2.7	0.994	259.304	1.6	0.998
0.55	289.780	3.1	0.988	257.818	1.6	0.998
0.6	288.823	4.5	0.990	253.631	1.6	0.998
0.65	285.350	2.2	0.996	252.868	1.7	0.997
0.7	283.466	2.9	0.995	245.196	1.8	0.997
0.75	282.830	3.1	0.994	242.410	2.0	0.996
0.8	276.619	2.9	0.994	237.708	1.6	0.998
0.85	262.108	2.5	0.996	-	-	-
Mean	265.716	3.01	0.994	248.660	1.9	0.997

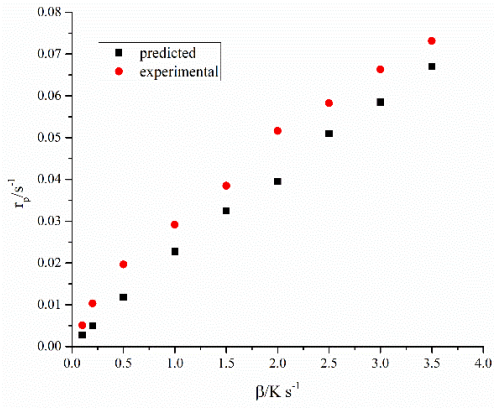

Fig. 6 Dependence of r_p on β for red XPS

The experimental peak reaction rates from (18) were compared with the predicted peak reaction rates from (26) by evaluating the dependence of peak reaction rate on heating rate. Plots of peak reaction rate versus heating rate obtained for red and grey XPS are illustrated in Figs. 6 and 7. According to (18), as well as Figs. 6 and 7, the peak reaction rate increased linearly with increasing heating rate. Also, the error margin between the predicted and experimental peak reaction rates was observed to be small in grey XPS as compared with red XPS.

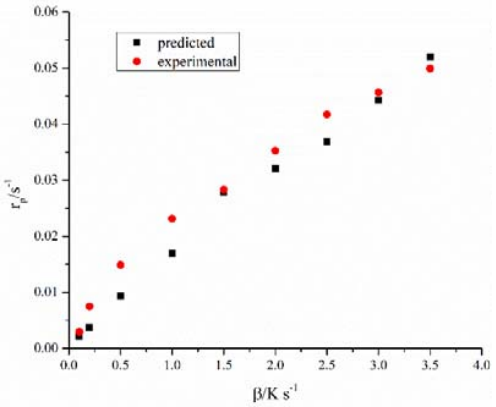

Fig. 7 Dependence of r_p on β for grey XPS

TABLE V
THE DEPENDENCE OF E_a ON A FROM MCC ANALYSIS

Conversion	Grey XPS			Red XPS		
	E_a/kJ mol^{-1}	Standard error	R^2	E_a/kJ mol^{-1}	Standard error	R^2
0.1	272.435	1.47	0.993	320.379	3.8	0.993
0.15	256.382	0.92	0.998	317.149	1.2	0.992
0.2	250.372	0.47	0.998	283.014	0.9	0.995
0.25	242.694	0.62	0.997	266.151	0.6	0.997
0.3	245.609	0.41	0.998	255.816	0.7	0.996
0.35	239.286	0.53	0.997	243.342	0.5	0.998
0.4	233.908	0.43	0.997	236.192	0.5	0.998
0.45	233.635	0.42	0.998	234.376	0.3	0.999
0.5	230.867	0.55	0.998	223.685	0.3	0.999
0.55	227.686	0.32	0.999	220.935	0.4	0.998
0.6	226.242	0.33	0.999	220.476	0.3	0.999
0.65	224.505	0.21	0.999	219.603	0.3	0.999
0.7	223.309	0.42	0.998	217.275	0.3	0.999
0.75	221.989	0.31	0.999	216.578	0.6	0.999
0.8	220.248	0.21	0.999	215.037	0.23	0.999
0.85	219.948	9.21	0.999	213.588	0.3	0.999
0.9	219.524	0.36	0.998	212.871	0.3	0.999
Mean	234.626	1.01	0.998	242.145	0.7	0.998

TABLE VI
THE DEPENDENCE OF E_a ON A FROM TG ANALYSIS

Conversion	Red XPS			Grey XPS		
	E_a/kJ mol^{-1}	Standard error	R^2	E_a/kJ mol^{-1}	Standard error	R^2
0.1	129.964	5.3	0.95	154.536	2.264	0.952
0.15	250.731	2.95	0.98	219.681	3.53	0.943
0.2	281.349	7.1	0.954	254.404	4.41	0.934
0.25	290.849	7.09	0.988	281.866	3.685	0.961
0.3	322.047	5.98	0.925	273.246	3.14	0.97
0.35	317.792	4.98	0.942	273.183	2.988	0.972
0.4	315.941	5.3	0.939	271.181	2.735	0.977
0.45	292.978	4.88	0.938	262.474	2.956	0.971
0.5	291.831	4.5	0.945	259.008	2.73	0.973
0.55	288.137	4.81	0.938	254.685	2.674	0.975
0.6	285.624	4.2	0.952	253.720	2.7	0.973
0.65	284.254	4.309	0.949	245.464	2.93	0.966
0.7	278.893	4.02	0.953	242.617	3.05	0.964
0.75	269.950	4.29	0.944	237.416	3.59	0.948
0.8	263.517	4.5	0.936	224.099	2.797	0.973
0.85	210.938	5.32	0.974	-	-	-
Mean	269.12	4.97	0.950	247.172	3.08	0.963

D.Derivation of E_a with FWO and KAS Methods

The KAS and FWO iso-conversional methods were applied in obtaining the activation energies for the degradation processes. Both heat release and mass loss kinetics for red and grey XPS were analyzed within a conversion range of 0.1 and 0.9. The dependence of the activation energy values obtained by the FWO method on the extent of conversion from the results of TG and MCC analysis is presented in Tables IV and V. From these tables, the apparent activation energy for red XPS was 265 kJ mol^{-1} and 242 kJ mol^{-1} from TG and MCC, respectively. On a similar note, 248 kJ mol^{-1} and 234 kJ mol^{-1} were recorded for TG and MCC kinetic analysis of grey XPS.

The activation energy data obtained for TG and MCC from the KAS method are presented in Tables VI and VII, respectively. According to the results, red XPS had higher activation energy values with an average of 269.12 kJ mol^{-1} for TG and 243 kJ mol^{-1} for MCC. However, the activation energy recorded for grey XPS was lower compared to the results for red XPS. A value of 247 kJ mol^{-1} was attained from TG while 235 kJ mol^{-1} was obtained from the mass loss kinetics.

A comparison was made between the activation energy results from FWO and KAS methods to evaluate the consistency and accuracy in Figs. 8 and 9. From the figures, similar trends were observed for the two methods in both TG and MCC. It was, however, quite clearly seen in Fig. 8 that at lower conversions of the TG analysis, the activation energy curves for red XPS were wide apart whiles similar values were obtained at higher conversion. The analysis was considered to

be accurate following the comparable average activation energies attained. It can also be observed from the figures that at each conversion, the Ea required was higher for red XPS. Practically, the energy required for a reaction to occur in red XPS is higher than in grey XPS. Red XPS has a longer burning time, releases more heat and has a higher mass loss rate than grey XPS. Therefore, it is easier for grey XPS to degrade thermally. This explains the lower kinetic parameters attained for grey XPS.

It was rather very obvious that Ea in the present study was higher than the reported values in literature [6], [7]. The higher Ea values could be attributed to the higher heating rates applied in the experiments. At higher heating rates, the samples are subjected to higher temperature gradients which may require higher Ea. This affirms the premise that activation energies increase with increasing heating rates.

TABLE VII
THE DEPENDENCE OF E_A ON A FROM MCC ANALYSIS

Conversion	Grey XPS			Red XPS		
	E_a/kJ mol^{-1}	Standard error	R^2	E_a/kJ mol^{-1}	Standard error	R^2
0.1	275.319	2.29	0.963	326.045	2.45	0.936
0.15	258.316	1.45	0.983	322.403	1.91	0.992
0.2	251.909	0.75	0.995	286.379	1.32	0.995
0.25	246.789	0.97	0.991	268.541	0.93	0.997
0.3	243.776	0.66	0.996	257.581	1.15	0.995
0.35	240.073	0.86	0.993	244.375	0.81	0.994
0.4	234.379	0.89	0.992	236.719	0.52	0.999
0.45	234.059	0.71	0.995	234.814	0.78	0.997
0.5	231.106	0.69	0.995	223.514	0.51	0.998
0.55	227.713	0.52	0.997	220.568	0.72	0.997
0.6	226.126	0.55	0.997	220.019	0.51	0.999
0.65	224.341	0.34	0.998	219.046	0.53	0.999
0.7	222.960	0.70	0.995	217.063	0.44	0.999
0.75	221.620	0.50	0.997	215.476	0.55	0.998
0.8	219.693	0.36	0.999	214.182	0.55	0.998
0.85	219.251	0.62	0.995	212.521	0.40	0.999
0.9	218.878	0.68	0.995	211.838	0.46	0.999
Mean	235.077	0.8	0.993	243.005	0.85	0.994

TABLE VIII
DEGREE OF DEVIATION BETWEEN THE ACTIVATION ENERGY FROM MCC AND TG

Iso-conversional method	Material	Deviation/ kJ mol^{-1}
KAS	Red XPS	22.1
	Grey XPS	12.09
FWO	Red XPS	23.6
	Grey XPS	14.03

We observed from the kinetic analysis that MCC results of both red XPS and grey XPS displayed lower activation energies as compared to the TG analysis experiments. The degrees of deviation of MCC from TG for the iso-conversional methods considered are listed in Table VIII. A difference of about 22.1/23.6 kJ mol^{-1} was recorded for red XPS whereas 12.09/14.03 kJ mol^{-1} difference was observed for grey XPS from the kinetic analysis made by the KAS and FWO methods respectively. The deviation obtained could be said to be insignificant when compared to the average E_a for both experiments. Thus, for red XPS and grey XPS, the average activation energies required for thermal degradation are the same in TG and MCC affirming the kinetic analysis of polystyrene conducted in [15], [16]. We also deduced from the analysis that the difference between the activation energies was smaller for the less dense material (grey XPS) and vice versa.

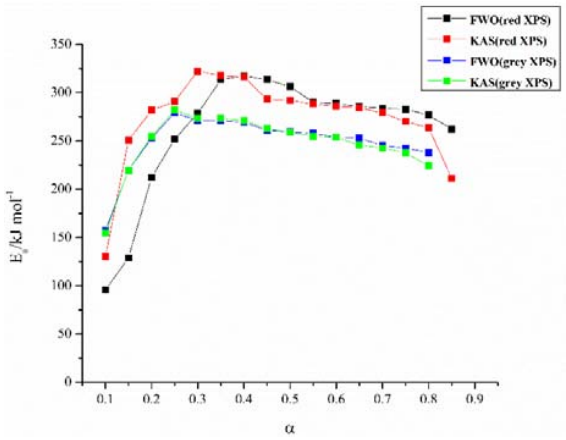

Fig. 8 Dependencies of the activation energy from TG on extent of conversion determined by KAS and FWO iso-conversional methods

A comparison was also made to evaluate the variation of activation energy profiles from TG and MCC experiments. E_a for TG pyrolysis increased steadily from the initial stages of degradation to the peak mass loss stage (at lower conversions thus $\alpha \leq 0.4$) indicating the possibility of parallel reactions during chain scission. At higher conversions ($\alpha > 0.4$), there was a gradual decrease in E_a signifying a relatively weak variation of the activation energy with conversion at the final stage.

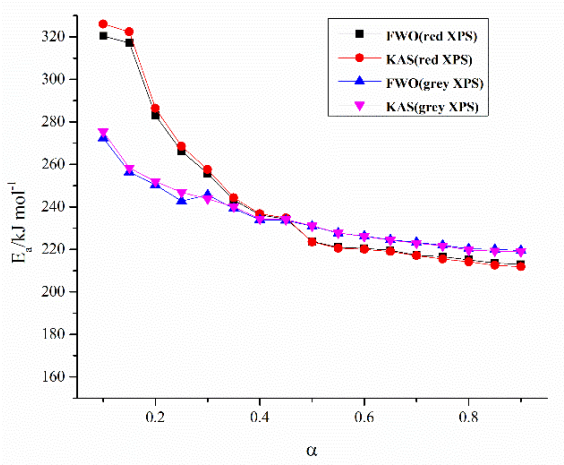

Fig. 9 Dependencies of the activation energy from MCC on extent of conversion determined by KAS and FWO iso-conversional methods

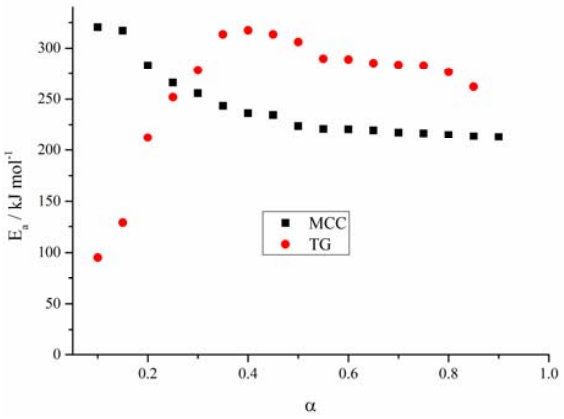

Fig. 10 Variation of E_a from MCC and TG for red XPS

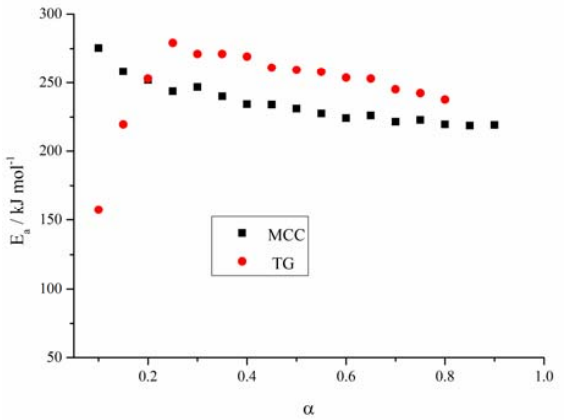

Fig. 11 Variation of E_a from MCC and TG for grey XPS

Unlike the degradation process in TG, a quite different trend was observed in the MCC results. It was observed in Tables V and VII as well as Figs. 10 and 11 that, Ea decreased rapidly from a peak of 326.1/320.4 and 275.3/272.4 kJ mol^{-1} for red XPS and grey XPS, respectively, at $0.1 \leq \alpha \leq 0.45$. This was followed by a gradual decrease showing a poor dependence of activation energy on the extent of conversion. The shape of the curve for the MCC analysis indicates a change in the rate determining step of the reaction. Consequently, it is quite evident that the polymers decomposed in different chemical pathways in both experiments. The different trends in activation energy profiles from MCC and TG demonstrated in Figs. 10 and 11 occurred as a result of the different pyrolysis processes used.

The dependence of the activation energy on the extent of conversion reveals the minimum number of elementary reactions that define the entire pyrolysis of a material. Therefore, to acquire the individual reactions that characterize the thermal degradation of a material, the kinetic analysis from both TG and MCC is required. However, since the apparent activation energy from both experiments are equivalent, any of the microscale experiments could be used for activation energy evaluation.

IV. Conclusion

The thermal degradation kinetics of red XPS and grey XPS were explored using TG and MCC experiments. Unlike the kinetic study in literature, the TG experiments were performed under higher heating rates ranging from 0.1-3.5 K/s. From the experiments, two mass loss stages were observed for both materials. Red XPS had higher heat release rate and smaller residual mass as compared to grey XPS. The peak reaction rates for the materials calculated from the MCC results had linear relationships with heating rate. The KAS and FWO methods were applied in obtaining the mass loss and heat release activation energies for the two XPS samples. The study presented low activation energies for grey XPS. Also, the activation energies calculated from the MCC results were lower than that of TG. From the kinetic analysis, the differences between the average activation energies for TG and MCC for both materials were insignificant. It was however obvious that different chemical pathways were used for the pyrolysis considering the different activation energy profiles demonstrated. It was concluded from this study that both MCC and TG experimental results are required to obtain the individual elementary reactions for a pyrolysis process.

Acknowledgment

This research is supported by the National Natural Science Fund of China, No.51776098; and the Fundamental Research Funds for the Central Universities, No.30918015101.

References

[1] Keattch, CJ, Dollimore D (2000). An introduction to thermogravimetry. Heyden.
[2] ASTM E1641-16 (2016), Standard Test Method for Decomposition Kinetics by Thermogravimetry Using the Ozawa/Flynn/Wall Method, ASTM International, West Conshohocken, PA.
[3] Prime RB, Bair HE, Vyazovkin S, Gallagher PK, Riga A (2009). Thermogravimetric analysis (TG). Thermal analysis of polymers: Fundamentals and applications. 241-317.
[4] Kim, E., & Dembsey, N. (2012). Engineering guide for estimating material pyrolysis properties for fire modeling. Project Final Report, 382.

[5] Matala A, Lautenberger C, Hostikka S (2012). Generalized direct method for pyrolysis kinetic parameter estimation and comparison to existing methods. Journal of fire sciences. 30(4):339-56.
[6] Jiang L, Zhang D, Li M, He JJ, Gao ZH, Zhou Y, Sun JH. (2018). Pyrolytic behavior of waste extruded polystyrene and rigid polyurethane by multi kinetics methods and Py-GC/MS. Fuel, 222, 11-20.
[7] Jiao LL, Sun JH (2014). A thermal degradation study of insulation materials extruded polystyrene. Procedia Engineering, 71, 622-628.
[8] Mishra RK, Mohanty K (2018). Pyrolysis kinetics and thermal behavior of waste sawdust biomass using thermogravimetric analysis. Bioresource technology. 251:63-74.
[9] Lyon, R. E., & Walters, R. N. (1999). U.S. Patent No. 5,981,290. Washington, DC: U.S. Patent and Trademark Office.
[10] Walters RN, Lyon RE (2001), Heat release capacity. Fire & Materials Conference, San Francisco, CA.
[11] Lyon RE, Walters RN (2004), Pyrolysis combustion flow calorimetry. Journal of Analytical and Applied Pyrolysis. 71(1):27-46.
[12] Walters R.N, Lyon R.E (1997), Microscale combustion calorimeter for determining flammability parameters of materials. Evolving Technologies for the Competitive Edge. 42: 1335-1344.
[13] Asante-Okyere, S., Xu, Q., Mensah, R. A., Jin, C., & Ziggah, Y. Y. (2018). Generalized regression and feed forward back propagation neural networks in modelling flammability characteristics of polymethyl methacrylate (PMMA). Thermochimica Acta, 667, 79-92.
[14] Mensah, R. A., Xu, Q., Asante-Okyere, S., Jin, C., & Bentum-Micah, G. Correlation analysis of cone calorimetry and microscale combustion calorimetry experiments. Journal of Thermal Analysis and Calorimetry, 1-11.
[15] Snegirev AY, Talalov VA, Stepanov VV, Harris JN (2012). Formal kinetics of polystyrene pyrolysis in non-oxidizing atmosphere. Thermochimica acta. 548:17-26.
[16] Snegirev, A. Y. (2014). Generalized approach to model pyrolysis of flammable materials. Thermochimica Acta, 590, 242-250.
[17] Standard Test Method for Determining Flammability Characteristics of Plastic's and Other Solid Materials Using Microscale Combustion Calorimetry. ASTM D7309-13.
[18] Lyon RE, Walters RN (2004). Pyrolysis combustion flow calorimetry. Journal of Analytical and Applied Pyrolysis. 71(1):27-46.
[19] Brems A, Baeyens J, Beerlandt J, Dewil R (2011). Thermogravimetric pyrolysis of waste polyethylene-terephthalate and polystyrene: A critical assessment of kinetics modelling. Resources, Conservation and Recycling. 55(8):772-81.
[20] Logan SR. (1982). The origin and status of the Arrhenius equation. Journal of Chemical Education, 59(4), 279.
[21] Chen Y, Wang Q (2007) Thermal oxidative degradation kinetics of flame-retarded polypropylene with intumescent flame-retardant master batches in situ prepared in twin-screw extruder. Polymer Degradation and Stability. 92:280–91.
[22] Bianchi O, Oliveira R, Fioro R, Martins J, Zattera A, Canto L (2008). Assessment of Avrami, Ozawa and Avrami–Ozawa equations for determination of EVA cross-linking kinetics from DSC measurements. Polymer Testing. 27:722–9.
[23] Lyon RE, Filipczak R, Walters RN, Crowley S, Stoliarov SI (2007). Thermal Analysis of Polymer Flammability, Report No. DOT/FAA/AR-07/2.
[24] Akahira T, Sunose T (1971). Method of determining activation deterioration constant of electrical insulating materials. Res Rep Chiba Inst Technol (Sci Technol). 16:22–31.